Modeling of terahertz radiation absorption temperature distribution in biological tissue of a cattle using Simulink-MATLAB model

Dewi Kurnia[1],*, Muhammad Hamdi[1], Juandi Muhammad[1], Saktioto[1], Preecha Yupapin[2,3], Hewa Yaseen Abdullah[4,5]

[1]Department of Physics, Universitas Riau, Pekanbaru 28293, Indonesia
[2]Department of Electrical Technology, IVNE - Region 2, Sakon Nakhon 47000, Thailand
[3]Computational Optics Research Group, Van Lang University, Ho Chi Minh City 713000, Viet Nam
[4]Research Center, Salahaddin University, Erbil 44002, Iraq
[5]Department of Physics Education, Tishk International University, Erbil 44001, Iraq

ABSTRACT

Terahertz radiation (THz) has interesting and effective properties in the field of biomedical imaging techniques, this is because of its ability to interact easily, is not ionized, and does not damage biological tissue. The purpose of this study was to determine the effect of THz radiation power density on temperature distribution and heat production in bovine biological tissue consisting of skin, fat, and muscle using a modeling approach. This study uses biophysical computation techniques with the Simulink-MATLAB model in the 0.1 – 1 THz frequency range, 50 – 150 mW power, and 5 – 25 mW/mm³ power density. Temperature distribution modeling is carried out in two ways, namely with different power densities and variations in the circumference of the THz radiation source. The results showed that the higher the power density used, the greater the absorbed radiation energy with increasing temperature. This causes the temperature distribution in the biological tissue to be wider and the production of heat in the tissue will increase. The results of imaging analysis of temperature distribution to depth in bovine biological tissue, show that fat tissue has less heat production compared to other tissues. The comparison of experimental data and modeling results shows an error percentage of 1.09%.

ARTICLE INFO

* Corresponding Author
E-mail address: dewikurnia119@gmail.com

1. INTRODUCTION

THz radiation has more interesting and meaningful properties in the field of biomedical imaging techniques than infrared radiation [1]. THz radiation has low scattering properties of tissue, making it negligible [2]. The photon energy of THz radiation is relatively lower than X-ray radiation so that it is not ionized by biological tissue and is safe to use [3, 4]. Heat control in biological tissue is important for maintaining body condition [5], therefore it is very important to have an accurate model for imaging the temperature distribution of THz radiation in biological tissue. This research applies biophysical computation techniques using the Simulink-MATLAB model with the Wolfram Mathematica 9.0 application.

The biophysical computational technique is an electronic differential analysis mechanism that studies and analyzes a dynamic model to determine physical parameters that can be designed using mathematical software [6]. The mathematical software model used in this study is the Simulink-MATLAB model can make simulations in the form/mathematical system model [7]. Imaging is done using an Wolfram Mathematica 9.0 application. Application Wolfram Mathematica is a modern technical computing system that covers most areas of technical computing, including neural tissue,

machine learning, image processing, geometry, data science, visualization, and others [8-11]. The biophysical computation technique with the Simulink-MATLAB model in this study is used to solve Maxwell's basic equations and the bioheat model for modification and calculation of the scattering factors that affect the volume unit heat production rate in tissue cells. This imaging technique designs a mathematical model for the absorption of terahertz radiation fields and heat changes in the bovine biological tissue layers. This study uses a frequency range of 0.1 – 1.0 THz with a power of 100 – 150 mW and a power density of 5 – 20 mW/mm^3. Using the Simulink-MATLAB model with the Wolfram Mathematics 9.0 application to see influence absorption of THz radiation by bovine biological tissue on temperature distribution through modeling using physical parameters. This modeling can analyze the effect of penetrating power of THz radiation in biological tissue by analyzing the scattering of radiation, which depends on the angle and wavelength using THz frequency and sub-millimeter wavelength in the range from 0.1 – 3 mm [12]. The power density (mW/mm^3) is an important parameter because the interaction between THz radiation and the tissue involves the absorption and spread of photon radiation. When THz radiation penetrates the sample tissue, the effect is scattering and absorption by polarized molecules [13].

The compartment theory for the rate of energy Q in biophysics considers the substance of the tissue structure as an interesting analogy that can explain into a compartment partition concept, so there is a main compartment that functions as an integrator. This integrator is a terminal process for the input and output of heat flow in the skin, fat, tumor, and muscle tissue caused by the specific application rate (SAR) of THz radiation which is connected to the radiation electric field, so that the temperature will rise during the radiation of THz radiation in the tissue [14, 15].

$$SAR = \frac{2\mu_t \sigma E^2 T}{\pi \rho \delta \omega^2} \exp\left(-\frac{2r^2}{\omega^2}\right) \exp\left(-\frac{\mu_t z}{\delta}\right) \tag{1}$$

The influencing parameters include electrical conductivity σ (S/mm), mass density ρ (kg/m), total absorption and scattering attenuation coefficient $\mu = \mu_a + \mu_s$ (mm^{-1}), the diameter of THz source circumference ω (mm), optical density δ (mm), distance of power source to tissue surface r (cm), radiation electric field THz E (V/mm).

This study uses Maxwell's equations to determine the initial and boundary conditions of the biological tissue temperature in the model [5, 15, 16].

$$\frac{\partial E}{\partial t} = \nabla^2 E + \sum_{i=1}^{N} K_i Q_i(E, H, x, T), \quad t > 0, 0 < x < L \tag{2}$$

$$\frac{\partial H}{\partial t} = \nabla^2 H + \sum_{i=1}^{N} K_i Q_i(E, H, x, T), \quad t > 0, 0 < x < L \tag{3}$$

$$\frac{\partial T}{\partial t} = \nabla^2 T + \sum_{i=1}^{N} K_i Q_i(E, H, x, T), \quad t > 0, 0 < x < L \tag{4}$$

$$T_{1i+1} = T_{1i} + \frac{1}{6}(K_1 + 2K_2 + 2K_3 + K_4) \tag{5}$$

Equations (2) to (4) are the initial and boundary conditions of the equation representing the requirements for the solution which solves the bio-heat equation by entering the reflection factor. These equations are used when the temperature distribution is the same which implies the physical properties of the system are constant within the system boundaries. These equations will be solved using the Simulink-MATLAB method with analog computer systematic diagrams for differential analysis of these equations. Equations (2) to (4) are solutions for determining temperature T which is highly dependent on the value of the thermal conductivity parameters (K_1, K_2 to K_i) which are derived from experimental data. The parameter values of K_1, K_2 to K_i certainly bring some uncertainty from the experimental results used to measure temperature T [16, 17]. To get the value of K_i with an insignificant level of uncertainty, we must use Equation (5) which is the fourth order Runge-Kutta equation.

2. RESEARCH METHODS

The research method was carried out in a biophysical computation using the mathematical based Simulink-MATLAB model. This research was conducted in several stages as shown in Figure 1.
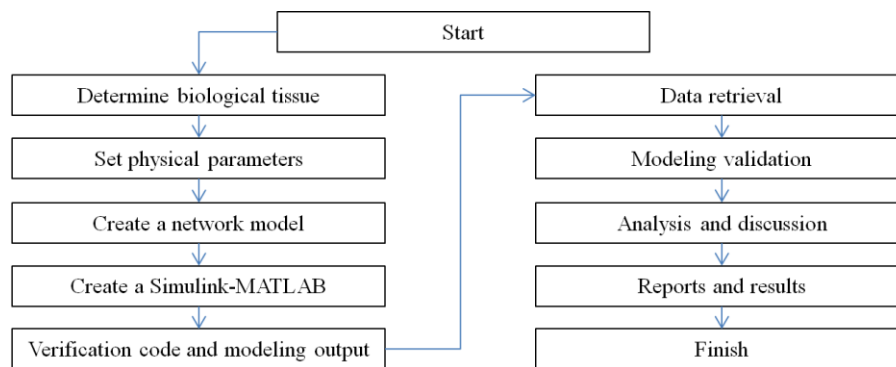

Figure 1. Diagram of the research stage of temperature distribution modeling.

2.1. Determining Biological Tissue

The tissue samples selected were normal and abnormal tissue from bovine tissue, namely skin, fat, tumor, and muscle tissue. Based on secondary data, namely experimental data from research done previously [18]. Parameters from THz radiation and biological tissue are used to see the interaction between THz radiation on the tissue using analog computer techniques using a mathematical-based Simulink-MATLAB model, namely the Wolfram Mathematica 9.0 application.

2.2. Setting Tissue Parameters

Determine the parameters used for modeling the temperature distribution and heat mapping of THz radiation absorption to biological tissue using the Simulink-MATLAB model. Table 1 shows the biological tissue parameters of bovine and Table 2 shows the parameters of THz radiation related to the modeling and is used to see the effect of THz radiation absorption on the temperature distribution in the depth of the bovine biological tissue.

Table 1. Biological tissue parameters [19-24].

Parameter type	Score
Frequency range	0.1 – 1 THz
Power range	10 – 500 mW
Timespan	Picosecond-minutes
Wavelength	300 – 3000 μm
Wave numbers	1 – 100 cm^{-1}
Tissue geometry	Rectangle
Tissue type	Skin, fat, muscle, tumor, cancer
Quantum energy	0.01 – 100 MeV
Thickness	1 – 25 mm
Absorption coefficient (CW)	23.5 – 100 cm^{-1}
Absorption coefficient (FTIR)	58.5 – 500 cm^{-1}

Table 2. THz radiation parameter [25].

Parameter	Score	Unit
Wavelength	50 – 240	mm
Credit dusasi	50	Ps
Pulse repetition frequency	2.8 – 11.2	MHz
Average power	400	W
Peak power	1	mW
The minimum relative width of the spectral line	3×10^{-3}	-
Average power density	1.4	W/cm^2

Modeling of terahertz radiation absorption temperature distribution ... (**Kurnia et al.**)

2.3. Creating a Biological Tissue Model

This bovine biological tissue model can explain the significant changes in thermal distribution that occur on the surface of normal and abnormal tissue layers caused by the effect of penetration of THz radiation on tissue depth, with influencing factors such as scattering, absorption, reflection, refraction, and dispersion such as shown by Figure 2.
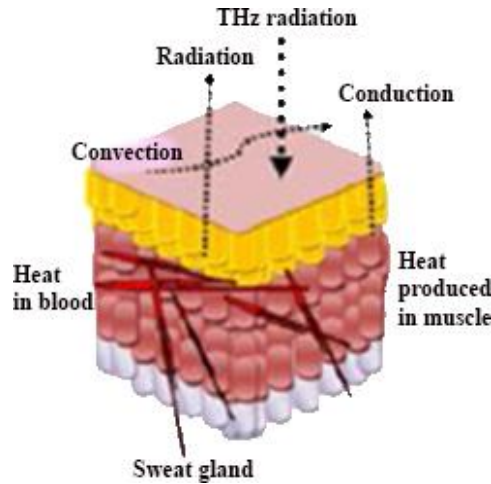

Figure 2. Interaction of THz radiation in bovine biological tissue layer model.

Absorption of THz radiation by the tissue in Figure 2 can cause an increase in hot temperature if there is no response from the parts of the tissue so what needs to be considered is the change in temperature through the input of heat sources, so it will be known how changes in tissue temperature ΔT and THz Q radiation energy source in response absorption and scattering of pulses.

2.4. Creating a Simulink-MATLAB Program

The program used for modeling the temperature distribution is Simulink-MATLAB with the Wolfram Mathematica 9.0 application. This program is applied to analyze through a Simulink-based dynamic system with a model made through analog circuit steps.
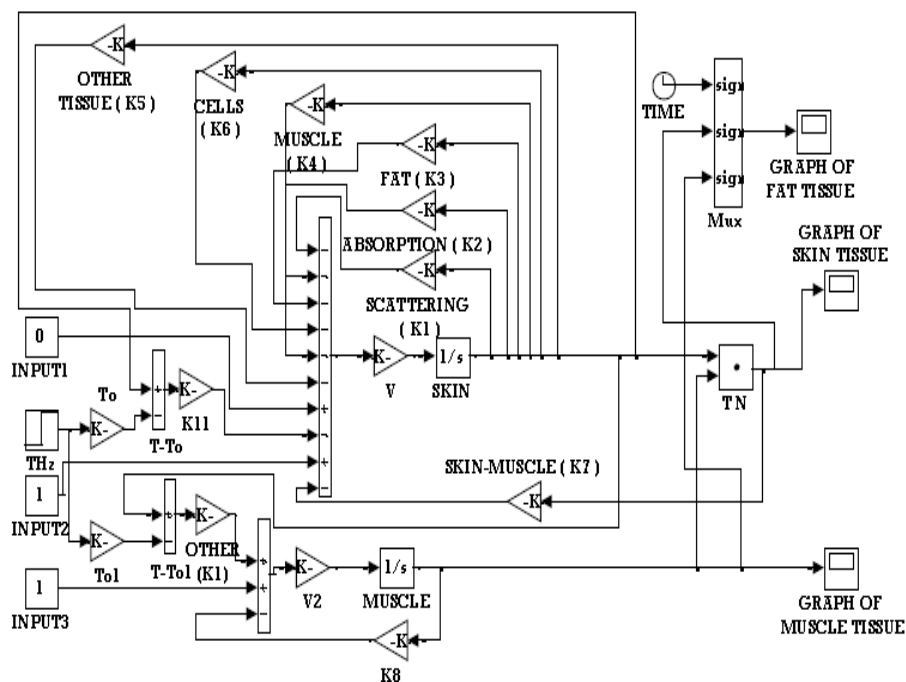

Figure 3. Simulink-MATLAB block diagram system thermal distribution of biological tissue.

Making the program starts from making a temperature distribution block diagram using the MATLAB program as shown in Figure 3. The program is tested whether it is successful or not, if it is successful then this program is transformed into a mathematical program so that it produces output in the form of a temperature distribution graph as shown in Figure 4. This graph is a graph of the temperature distribution to the depth of the tissue due to the absorption of THz radiation by the bovine biological tissue.
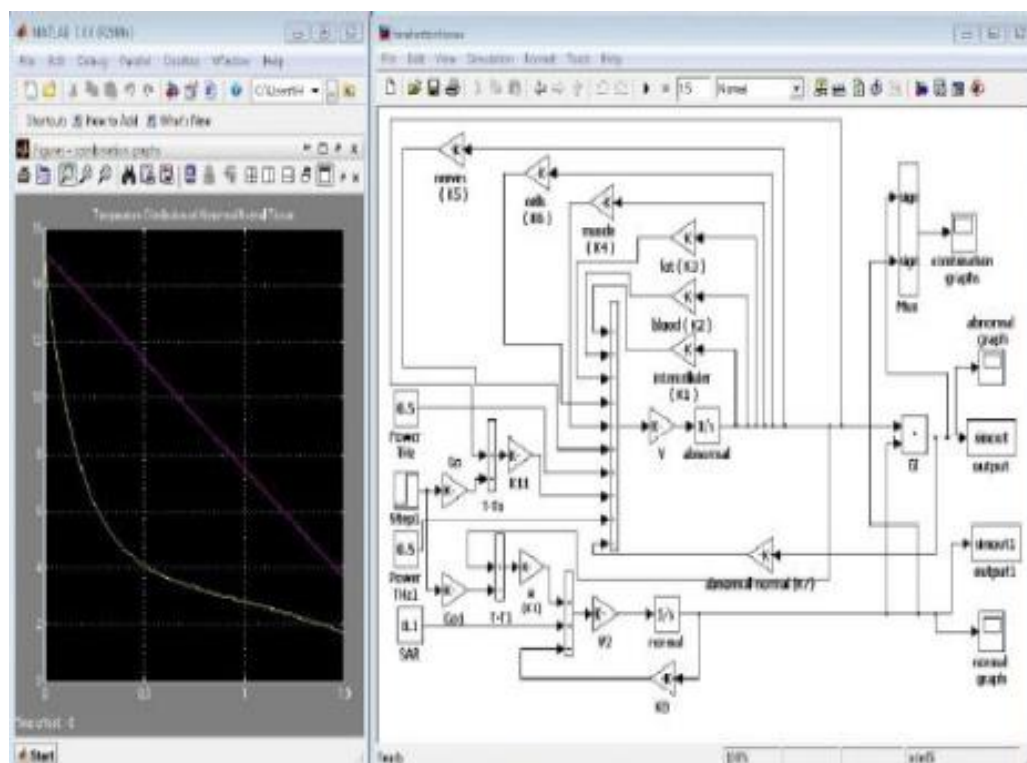

Figure 4. The output shape of the temperature distribution from the Simulink-MATLAB block diagram.

Figure 5 explains the next step, which is to create a temperature distribution modeling based program with the Simulink-MATLAB program using data from previous research experiments as secondary data and block diagrams that have been made. This program is then transformed into a mathematical program using the Wolfram Mathematica 9.0 application, resulting in a temperature distribution simulation program. This program is run according to the flowchart as shown in Figure 6.
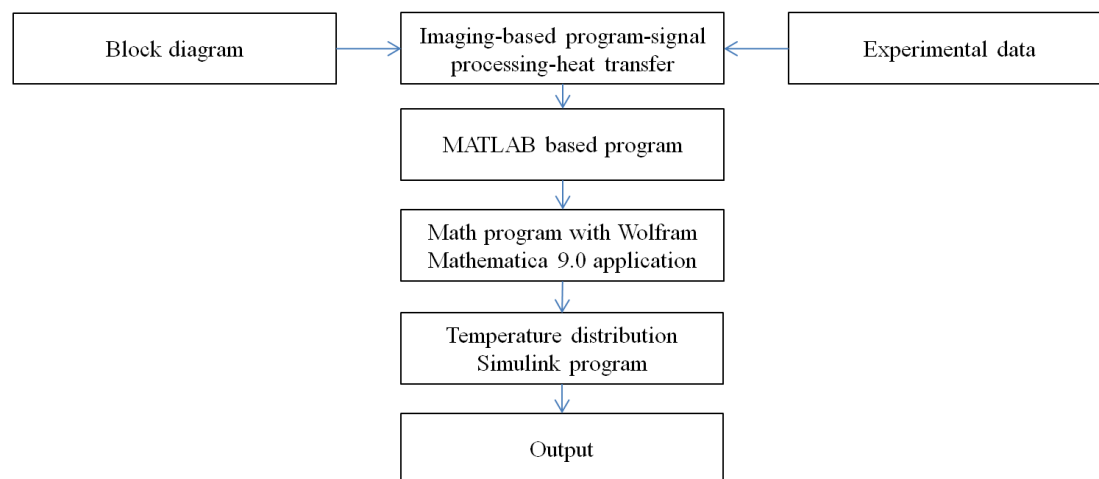

Figure 5. Flowchart of the process of implementing the Simulink-MATLAB system.
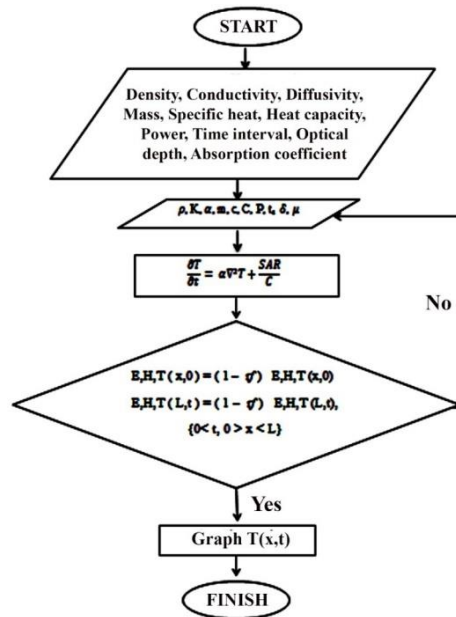
Figure 6. Flowchart of the temperature distribution of THz radiation absorption to bovine biological tissue.

3. RESULTS AND DISCUSSIONS

The data used in this study is the experimental data on the distribution of THz radiation absorption temperature to the biological tissue of bovine, namely skin, fat, tumor, and muscle tissue. The experimental data were then processed using the mathematical-based Simulink-MATLAB model with the Mathematica 9.0 program.

3.1. Modeling of Cattle Biological Tissue Temperature Distribution

Biological exposure to THz radiation in tissue can cause temperature distribution in the tissue. This temperature distribution is influenced by the heat conduction that occurs so that the temperature changes with the tissue depth shown in 1D.

3.2. Temperature Distribution Modeling with Changes in Tissue Parameters.

Analysis of temperature distribution using tumor tissue to see changes in temperature with tissue depth with changes in tissue parameters (see Figure 7).
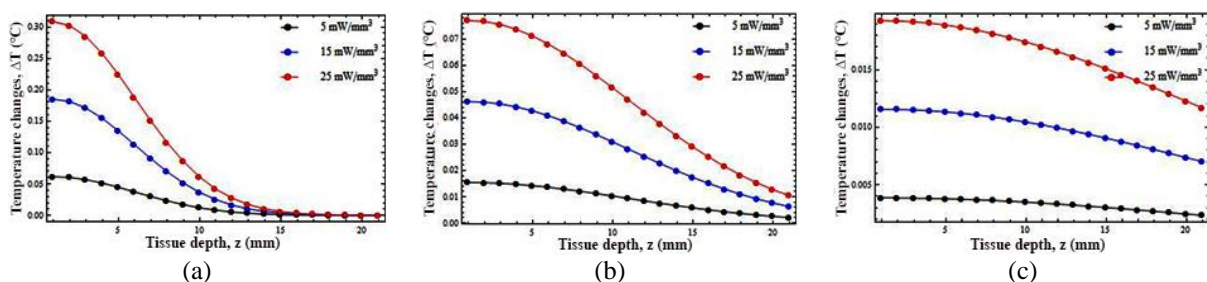

Figure 7. Modeling of THz radiation absorption temperature distribution with variations in the circumference of the THz source diameter: (a) 5 mm; (b) 10 mm; and (c) 20 mm.

Figure 7 shows that, if analyzed at the same power density, namely $S = 25$ mW/mm^3, the magnitude of the temperature change with the change in the diameter of the source circumference is when $wa = 5$ mm, $wb = 10$ mm, and $wc = 20$ mm respectively on $\Delta Ta = 0.31°C$, $\Delta Tb = 0.077°C$, and $\Delta Tc = 0.0195°C$, and so for the other power densities in each figure. This shows that the larger the circular diameter of the THz radiation source, the greater the energy emitted and will also affect changes in tissue temperature [18-20].

3.3. Absorption of THz Radiation on Heat Production of Biological Tissues

Absorption of THz radiation by biological tissue can cause heat conduction which affects the temperature distribution and heat production in the sample tissue.
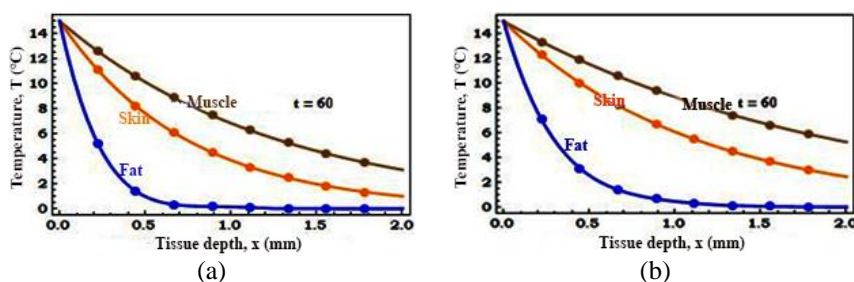

(a)	(b)

Figure 8. Heat production in biological tissue with radiation power: (a) 100 mW and (b) 150 mW.

Figure 8 (b) shows that at the time of exposure $t = 60$ s and the power of 150 mW the muscle tissue runs out of absorbed THz radiation energy, takes longer to zero point temperature (has greater heat production), then skin tissue, in contrast to fat tissue who experience significant temperature changes and experience faster exhaustion of absorbed THz radiation energy. This is because the fat tissue has a high water content with a more dilute concentration so that the THz radiation is absorbed very strongly which causes the radiation energy to decrease according to the greater penetration of the tissue depth in the fat tissue medium until the energy limit reaches zero, which means THz radiation energy will be lost during propagation in fat tissue [21, 22]. The absorption of THz radiation in fat tissue, skin, and muscle in the same duration of exposure, namely $t = 60$ s with different power 100 mW and 150 mW in Figure 8 (a) and (b) shows the difference in heat production in each tissue with different power. The amount of THz radiation power that is exposed to the tissue will make the heat production produced will also be greater. This causes the deep penetration of the absorbed THz radiation energy to take a long time to reach the temperature at zero [23-25].

3.4. Comparison of Experimental and Modeling Data.

Based on the comparison data of temperature changes to the depth of experimental results and modeling in Tables 3 it is obtained the average percentage error for each density power 5 mW/mm^3, 15 mW/mm^3, and 25 mW/mm^3 are 0.98%, 1.23%, and 1.05%. So it can be concluded that the error percentage of the modeling results is 1.09%.

Table 3. Comparison of changes in temperature results of experiments and modeling with variations power density S 5 mW/mm^3, 15 mW/mm^3, and 25 mW/mm^3.

Power Density ($S_1 = 5$mW/mm^3)			Power Density ($S_2 = 15$mW/mm^3)			Power Density ($S_3 = 25$mW/mm^3)		
Z (mm)	Change in Temperature ΔT (°C)	Error %	Z (mm)	Change in Temperature ΔT (°C)	Error %	Z (mm)	Change in Temperature ΔT (°C)	Error %
	Exp	Comp			Exp	Comp			Exp	Comp	

Z (mm)	Exp	Comp	Error %	Z (mm)	Exp	Comp	Error %	Z (mm)	Exp	Comp	Error %
0	0.062	0.062	0.00	0	0.187	0.189	0.01	0	0.312	0.315	0.01
1	0.046	0.059	0.28	1	0.139	0.165	0.19	1	0.23	0.29	0.26
2	0.034	0.048	0.41	2	0.103	0.14	0.36	2	0.17	0.245	0.44
3	0.025	0.038	0.52	3	0.076	0.115	0.51	3	0.13	0.205	0.58
4	0.019	0.03	0.58	4	0.056	0.1	0.79	4	0.09	0.165	0.83
5	0.014	0.025	0.79	5	0.042	0.083	0.98	5	0.07	0.127	0.81
6	0.01	0.02	1.00	6	0.031	0.075	1.42	6	0.05	0.1	1.00
7	0.008	0.017	1.13	7	0.023	0.062	1.70	7	0.038	0.085	1.24
8	0.006	0.015	1.50	8	0.017	0.055	2.24	8	0.029	0.075	1.59
9	0.004	0.013	2.25	9	0.013	0.045	2.46	9	0.021	0.065	2.10
10	0.003	0.01	2.33	10	0.009	0.035	2.89	10	0.016	0.06	2.75

4. CONCLUSION

Based on the data from the analysis of the temperature distribution of the absorption of THz radiation on biological tissue using the mathematical Simulink-MATLAB model, it can be concluded that the absorption of THz radiation by biological tissue with a large power density (S) causes the energy emitted to be greater so that the possibility of temperature changes at each point is greater and the resulting heat production will be greater. This is indicated by data $S_3 = 25$ mW/mm^3, $\Delta T = 0.30$°C; $S_2 = 15$ mW/mm^3, $\Delta T = 0.185$°C; and $S_1 = 5$ mW/mm^3, $\Delta T = 0.06$°C. Fat tissue has less heat production than skin and muscle tissue. This is because the fat tissue has a high water content with a more dilute concentration so that the THz radiation is absorbed very strongly which causes the radiation energy to decrease according to the greater tissue depth penetration in the fat tissue medium until the energy limit reaches zero. The comparison of the experimental and modeling data shows the values are not much different, where the error percentage is 1.09%. This shows that the analysis of the temperature distribution of THz radiation absorption in biological tissue using a mathematical-based Simulink-MATLAB model has a high degree of accuracy.

REFERENCES

[1] Romanenko, S., Begley, R., Harvey, A. R., Hool, L., & Wallace, V. P. (2017). The interaction between electromagnetic fields at megahertz, gigahertz and terahertz frequencies with cells, tissues and organisms: risks and potential. *Journal of The Royal Society Interface*, **14**(137), 20170585.

[2] Smolyanskaya, O. A., Chernomyrdin, N. V., Konovko, A. A., Zaytsev, K. I., Ozheredov, I. A., Cherkasova, O. P., Nazarov, M. M., Guillet, J. P., Kozlov, S. A., Kistenev, Y. V., Coutaz, J. L., Mounaix, P., Vaks, V. L., Son, J. -H., Cheon, H., Wallace, V. P., Feldman, Yu., Popov, I., Yaroslavsky, A. N., Shkurinov, A. P., & Tuchin, V. V. (2018). Terahertz biophotonics as a tool for studies of dielectric and spectral properties of biological tissues and liquids. *Progress in Quantum Electronics*, **62**, 1–77.

[3] Havariyoun, G., Vittoria, F. A., Hagen, C. K., Basta, D., Kallon, G. K., Endrizzi, M., Massimi, L., Munro, P., Hawker, S., Smit, B., Astolfo, A., Larkin, O. J., Waltham, R. M., Shah, Z., Duffy, S. W., Nelan, R. L., Peel, A., Suaris, T., Jones, J. L., Haig, I. G., Bate, D., & Olivo, A. (2019). A compact system for intraoperative specimen imaging based on edge illumination x-ray phase contrast. *Physics in Medicine and Biology*, **64**(23), 235005.

[4] Wahaia, F., Kasalynas, I., Venckevicius, R., Seliuta, D., Valusis, G., Urbanowicz, A., Molis, G., Carneiro, F., Silva, C. D. C., & Granja, P. L. (2016). Terahertz absorption and reflection imaging of carcinoma-affected colon tissues embedded in paraffin. *Journal of Molecular Structure*, **1107**, 214–219.

[5] Tay, Z. W., Chandrasekharan, P., Chiu-Lam, A., Hensley, D. W., Dhavalikar, R., Zhou, X. Y., Yu, E. Y., Goodwill, P. W., Zheng, B., Rinaldi, C., & Conolly, S. M. (2018). Magnetic particle imaging-guided heating in vivo using gradient fields for arbitrary localization of magnetic hyperthermia therapy. *ACS Nano*, **12**(4), 3699–3713.

[6] Mäki-Marttunen, T., Kaufmann, T., Elvsåshagen, T., Devor, A., Djurovic, S., Westlye, L. T., Linne, M. L., Rietschel, M., Schubert, D., Borgwardt, S., Efrim-Budisteanu, M., Bettella, F., Halnes, G., Hagen, E., Naess, S., Ness, T. V., Moberget, T., Metzner, C., Edwards, A. G., Fyhn, M., Dale, A. M., Einevoll, G. T., & Andreassen, O. A. (2019). Biophysical psychiatry—how computational neuroscience can help to understand the complex mechanisms of mental disorders. *Frontiers in psychiatry*, **10**, 534.

[7] Nikiforov, V. M. & Bykanov, I. Y. (2018). CAD-technology of «cross-cutting» design of dynamic systems. *2018 25th Saint Petersburg International Conference on Integrated Navigation Systems (ICINS)*, 1–4.

[8] Cioruța, B. V., Lauran, A., & Coman, M. (2020). Some analytical considerations regarding the traveling salesman problem solved with Wolfram Mathematica applications. *Asian Journal of Advanced Research and Reports*, **12**(1), 68–77.

[9] Fitriani, R., Muhammad, J., & Rini, A. S. (2020). Investigation of the Distribution of Aquifers and Groundwater Quality in the Village of Rimbo Panjang, Kampar District. *Science, Technology & Communication Journal*, **1**(1), 8–15.

[10] Pertiwi, M., Muhammad, J., Farma, R., & Saktioto, S. (2020). Analysis of Shallow Well Depth Prediction: A Study of Temporal Variation of GRACE Satellite Data in Tampan District-Pekanbaru, Indonesia. *Science, Technology & Communication Journal*, **1**(1), 27–36.

[11] Roslan, M. S., Chaudhary, K. T., Mazalam, E., & Saktioto, S. (2020). Overview of Temporal Soliton Transmission on Photonic Crystal Fiber and Nanowires. *Science, Technology & Communication Journal*, **1**(1), 16–19.

[12] Bao, C. Q., Truong, Anthony, J. F., Fan, S., & Wallace, V. P. (2018). Concentration analysis of breast tissue phantoms with terahertz spectroscopy. *Biomedical Optics Express*, **9**(3), 1334–1349.

[13] Al-Ibadi, A., Sleiman, J. B., Cassar, Q., Macgrogan, G., Balacey, H., Zimmer, T., Mounaix, P., & Guillet, J. P. (2017). Terahertz biomedical imaging: From multivariate analysis and detection to material parameter extraction. *2017 Progress in Electromagnetics Research Symposium-Spring (PIERS)*, 2756–2762.

[14] Franchini, V., De Sanctis, S., Marinaccio, J., De Amicis, A., Coluzzi, E., Di Cristofaro, S., Lista, F., Regalbuto, E., Doria, A., Giovenale, E., Gallerano, G. P., Bei, R., Benvenuto, M., Masuelli, L., Udroiu, I., & Sgura, A. (2018). Study of the effects of 0.15 terahertz radiation on genome integrity of adult fibroblasts. *Environmental and molecular mutagenesis*, **59**(6), 476–487.

[15] Spathmann, O., Schürmann, R., Zang, M., Streckert, J., Hansen, V., Saviz, M., & Clemens, M. (2018). Thermal impact on the human oral cavity exposed to radiation from biomedical devices operating in the terahertz frequency range. *Journal of Infrared, Millimeter, and Terahertz Waves*, **39**, 926–941.

[16] Madhukar, A., Park, Y., Kim, W., Sunaryanto, H. J., Berlin, R., Chamorro, L. P., Bentsman, J., & Ostoja-Starzewski, M. (2019). Heat conduction in porcine muscle and blood: experiments and time-fractional telegraph equation model. *Journal of the Royal Society Interface*, **16**(160), 20190726.

[17] Viswanath, V., Pantel, A. R., Daube-Witherspoon, M. E., Doot, R., Muzi, M., Mankoff, D. A., & Karp, J. S. (2020). Quantifying bias and precision of kinetic parameter estimation on the PennPET Explorer, a long axial field-of-view scanner. *IEEE Transactions on Radiation and Plasma Medical Sciences*, **4**(6), 735–749.

[18] Dong, J., Breitenborn, H., Piccoli, R., Besteiro, L. V., You, P., Caraffini, D., Wang, Z.M., Govorov, A. O., Naccache, R., Vetrone, F., Razzari, L., & Morandotti, R. (2020). Terahertz three-dimensional monitoring of nanoparticle-assisted laser tissue soldering. *Biomedical Optics Express*, **11**(4), 2254–2267.

[19] Breitenborn, H., Dong, J., Piccoli, R., Bruhacs, A., Besteiro, L. V., Skripka, A., Wang, Z.M., Govorov, A. O., Razzari, L., Vetrone, F., Naccache, R., & Morandotti, R. (2019). Quantifying the photothermal conversion efficiency of plasmonic nanoparticles by means of terahertz radiation. *APL Photonics*, **4**(12).

[20] Naccache, R., Mazhorova, A., Clerici, M., Piccoli, R., Khorashad, L. K., Govorov, A. O., Razzari, L., Vetrone, F., & Morandotti, R. (2017). Terahertz thermometry: combining hyperspectral imaging and temperature mapping at terahertz frequencies. *Laser and Photonics Reviews*, **11**(5), 1600342.

[21] Smolyanskaya, O. A., Schelkanova, I. J., Kulya, M. S., Odlyanitskiy, E. L., Goryachev, I. S., Tcypkin, A. N., rachev, Y. V., Toropova, Y. G., & Tuchin, V. V. (2018). Glycerol dehydration of native and diabetic animal tissues studied by THz-TDS and NMR methods. *Biomedical optics express*, **9**(3), 1198–1215.

[22] Zaytsev, K. I., Dolganova, I. N., Chernomyrdin, N. V., Katyba, G. M., Gavdush, A. A., Cherkasova, O. P., Komandin, G. A., Shchedrina, M. A., Khodan, A. N., Ponomarev, D. S., Reshetov, I. V., Karasik, V. E., Skorobogatiy, M., Kurlov, V. N., & Tuchin, V. V. (2019). The progress and perspectives of terahertz technology for diagnosis of neoplasms: A review. *Journal of Optics*, **22**(1), 013001.

[23] Guo, C., Guo, W., Xu, H., Zhang, L., Chen, G., D'Olimpio, G., Kuo, C.N., Lue, C.S., Wang, L., Politano, A., Chen, X., & Lu, W. (2020). Ultrasensitive ambient-stable SnSe2-based broadband photodetectors for room-temperature IR/THz energy conversion and imaging. *2D Materials*, **7**(3), 035026.

[24]   Saktioto, Zairmi, Y., Veriyanti, V., Candra, W., Syahputra, R. F., Soerbakti, Y., Asyana, V., Irawan, D., Hairi, H., Hussein, N. A., & Anita, S. (2020). Birefringence and Polarization Mode Dispersion Phenomena of Commercial Optical Fiber in Telecommunication Tissue. *Journal of Physics: Conference Series*, **1655**(1), 012160.

[25]   Ryu, M., Ng, S. H., Anand, V., Lundgaard, S., Hu, J., Katkus, T., Appadoo, D., Vilagosh, Z., Wood, A. W., Juodkazis, S., & Morikawa, J. (2021). Attenuated total reflection at THz wavelengths: prospective use of total internal reflection and polariscopy. *Applied Sciences*, **11**(16), 7632.